Molybdenum carbide water–gas shift catalyst for fuel cell-powered vehicles applications

Dong Ju Moon* and Jong Woo Ryu

Reaction Media Research Center, Korea Institute of Science & Technology, P.O. BOX 131, Cheongryang, Seoul 130-650, Korea

Received 9 June 2003; accepted 10 October 2003

Molybdenum carbide catalysts for water–gas shift (WGS) reaction were investigated to develop an alternate commercial LTS ($Cu\text{-}Zn/Al_2O_3$) catalyst for an onboard gasoline fuel processor. The catalysts were prepared by a temperature-programmed method and were characterized by N_2 physisorption, CO chemisorption, XRD and XPS. It was found that the Mo_2C catalyst showed higher activity and stability than the commercial LTS catalyst, even though both catalysts were deactivated during the thermal cycling runs. The optimum carburization temperature for preparing Mo_2C was in the range of 640–650 °C. It was found that the deactivation of the Mo_2C catalyst was caused by the transition of $Mo^{\delta+}$ ($IV < \delta^+ < VI$, MoO_xC_y), Mo^{IV} and Mo_2C on the surface of the Mo_2C catalyst to Mo^{VI} (MoO_3) with the reaction of H_2O in the reactant. It was identified that molybdenum carbide catalyst is an attractive candidate for the alternate $Cu\text{-}Zn/Al_2O_3$ catalyst for automotive applications.

KEY WORDS: WGS; LTS; $Cu\text{-}Zn/Al_2O_3$; Mo_2C; thermal cycling; fuel cell-powered vehicles.

1. Introduction

The hydrogen may be provided to the fuel cell in pure form, or one may generate hydrogen from hydrocarbons in a fuel processor. Onboard fuel processor is the most convenient method of supplying hydrogen in the absence of a suitable infrastructure for hydrogen. Fuel-process technologies generate hydrogen from hydrocarbons by either steam reforming or autothermal reforming [1–3]. This reforming step generates gases, which contain 8–12% CO besides H_2, CO_2, CH_4 and air. This CO must be converted with the help of steam to CO_2 and hydrogen via the water–gas shift (WGS) reaction before a preferential partial oxidation (PROX) can reduce the CO content to <10 ppm for the proton exchanged membrane (PEM) fuel cell [1–4].

The WGS reaction is one of the key catalytic stages in a fuel processor. Since the reaction is exothermic, the equilibrium CO conversion is highest at low temperatures. Consequently, a two-stage process is often used [4–6]. In industrial reactors, the Fe_3O_4-Cr_2O_3 catalyst was used for the high-temperature shift (HTS) and the $Cu\text{-}Zn/Al_2O_3$ catalyst was used for the low-temperature shift (LTS) reaction. The reaction is moderately exothermic with $\Delta H = -41.1\,\mathrm{kJ/mol}$ [5]. The water–gas shift reaction is usually carried out in two adiabatic shift reactors, the high-temperature shift reactor and the low-temperature shift reactor, separated with an intercooler in between. The existing commercial LTS catalyst, though highly active, was unsuitable for transportation applications because of its large size and weight, and the deactivation tendency of the copper-based catalysts under the severe conditions encountered in an automotive system. Copper-based catalysts also cannot be used at temperatures above about 250 °C, which further limits their utility [6–9]. Therefore, the development of high-performance WGS catalysts for integration with PEM fuel cells is very important.

Thirty years ago, a number of researchers had shown that some transition metal carbides, such as those of molybdenum [10,12] and tungsten [10,13,14], have catalytic behavior similar to the noble metals. Since the starting materials for the production of the transition metal carbides are abundant and cheap, it has been suggested that they can replace the scarce and expensive noble metals in catalysis. One of the major problems with the metal carbide catalysts has been the difficulty in producing them with high specific surface area. In the previous work [6–9], the author suggests that high surface area carbides are promising candidates for development as commercial water–gas shift catalysts.

In this work, we have studied the WGS reaction over molybdenum carbides catalysts with different carburization temperatures. The thermal cycling performance of the Mo_2C catalyst was compared with those of the commercial LTS catalyst.

2. Experimental

2.1. Catalysts

Molybdenum carbide catalysts were synthesized by the carburization of molybdenum oxide [7–10]. A molybdenum oxide (99.99%) was obtained from

* To whom correspondence should be addressed.
E-mail: djmoon@kist.re.kr

1011-372X/04/0100–0017/0

Sigma-Aldrich Chemicals. Carburization of the oxide was done in a temperature-programmed method using an equimolar mixture of CH_4 and H_2 in flowing 400 cc/min. Approximately 5 g of the oxide was loaded into the quartz straight-tube reactor. The temperature program for carburization consisted of linearly heating the oxide at a rate of 600 °C/h to 300 °C, then at 60 °C/h to the final carburization temperature. Following a 2-h soak period at the final temperature, the product was quenched to room temperature and kept for 4 h in a mixture of 1% O_2 in He in flowing 30 cc/min [8–9].

The commercial LTS catalyst for cleanup of CO was obtained from ICI in the form of pellets. The catalysts in this work were used in the form of powder with a mesh size of 120/230, after crushing.

2.2. Characterization of catalysts

BET surface area and pore-size distributions of catalysts were measured by N_2 physisorption. The active metal surface areas of the prepared catalysts were measured by CO chemisorption using a sorption analyzer [Quantachrome Co. Autosorb-1C]. The carburization temperature of molybdenum oxide was determined via thermal gravimetric analysis [TGA, Sindo Science Co., TGA 2050] in conjunction with X-ray diffraction (XRD) [Shimazdu Co., XRD-6000]. Structure of the catalysts before and after the reaction was analyzed by the XRD and XPS [SSI Science Co., 2803-S spectrometer].

2.3. WGS reaction

The schematic diagram of the WGS reactor is shown in figure 1. It consists of four sections: feed supply, preheater, WGS reactor and gas chromatography (GC) analysis sections. The gases were delivered by mass-flow controllers and H_2O was fed by a liquid-delivery pump [Young Lin Co., model M930]. The LTS reactor made up of Inconel 600 tube (0.0075m i.d. and 0.20 m length) was used in this study. The reaction temperature was controlled by a PID temperature controller and was monitored by a separated thermocouple placed in the catalyst bed. This arrangement was capable of ensuring accuracy of ±1 °C of the catalyst bed temperature. Unreacted H_2O was removed by an ice trap and then the gas effluent was analyzed by an on-line gas chromatograph (HP-6890 Series) equipped with thermal conductivity detector (TCD) and using a carbosphere column (0.0032 m o.d. and 3.048 m length, 80/100 meshes).

The catalytic activity for LTS reaction in the fixed-bed reaction system was measured at atmospheric pressure and at a temperature range of 200–300 °C. The WGS catalyst of 0.5 g was charged in the reactor. The Cu-Zn/Al_2O_3 catalyst was reduced at 200 °C in a mixture of 2% H_2 in N_2 balance for 4.5 h. The Mo_2C

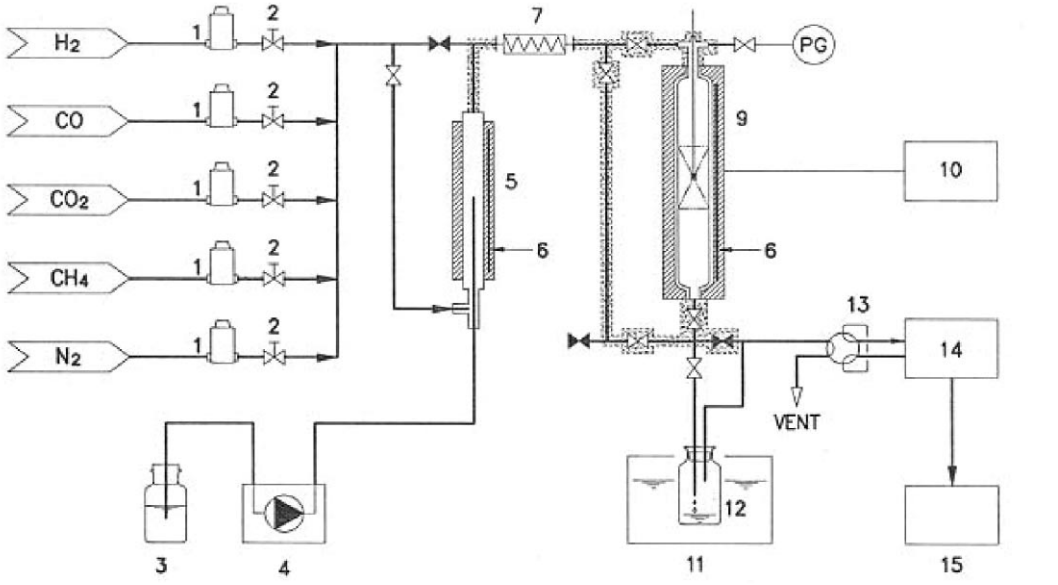

Figure 1. A schematic diagram of the WGS reaction system.

catalyst was reduced at 400 °C under the flow of H_2 for 4.5 h. The reactant gas contained 62.5% H_2 (99.999%), 31.8% deionized H_2O and 5.7% CO (99.999%).

3. Results and discussion

The characteristics of the prepared and the commercial LTS catalysts are summarized in table 1. It was found that the BET surface areas of Mo_2C catalysts (catalyst C, D and E) were similar to that of Cu-Zn/Al_2O_3 catalyst within an experimental error, while active metal surface area of Mo_2C was higher than that of the Cu-Zn/Al_2O_3 catalyst. It was observed that the BET surface areas of the carbide systems were greatly dependent on the carburization temperature. It was found that BET surface area of Mo_2C catalysts increased with increasing carburization temperatures from 615 to 640 °C and then fell.

The carburization temperature of molybdenum oxycarbides catalysts were investigated via thermal gravimetric analysis (TGA) in conjunction with XRD [9]. The TGA pattern for carburization of the oxide is shown in figure 2. The conversion of MoO_3 to Mo_2C occurs in two steps. The first event in the TGA pattern was produced a feature at room temperature to 580 °C. The weight loss associated with this event (12.2%) was consistent with the theoretical conversion of MoO_3 to MoO_2 (12.1%). The second event yielded a plateau starting at 610 °C. The total weight loss up to 615 °C (28.1%) was very close to the theoretical value for the conversion of MoO_3 to Mo_2C (29.1%). The formation of carbide phase begins at 580 °C and completes at 650 °C. For temperatures above 650 °C, excess of carbon deposits on the molybdenum carbide systems. Figure 3 shows the XRD patterns for molybdenum carbide catalysts with different carburization temperature. The transformation of MoO_3 to Mo_2C was well evidenced by XRD patterns of molybdenum-based catalysts with different carburization temperatures. It was found that the complete disappearance of molybdenum oxide phases, such as MoO_3 and MoO_2, occurs at the carburization temperatures above 640 °C.

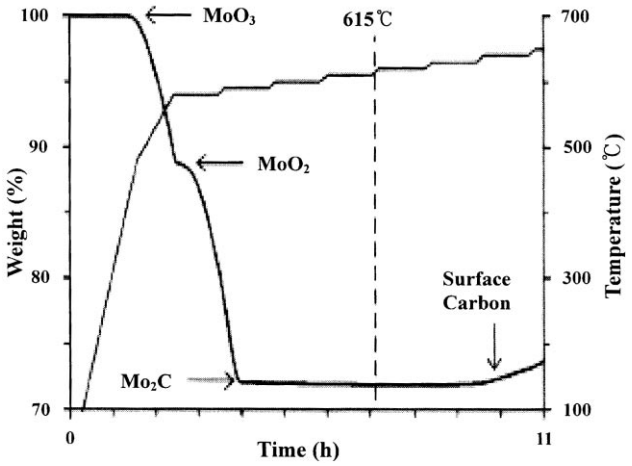

Figure 2. Thermal gravimetric analysis of the reaction of MoO_3 with an equimolar mixture of CH_4 and H_2 [9].

It was identified that molybdenum carbide catalysts ($\rho = 1.23$–$1.89\,g/cm^3$) have higher density than the commercial Cu-Zn/Al_2O_3 catalyst ($\rho = 1.1\,g/cm^3$). If molybdenum carbide catalysts showed higher gravimetric CO-consumption rate than the commercial LTS catalyst, Mo_2C catalyst is a more promising candidate than the commercial LTS catalyst because of the possibility of the reduction of the volume of the WGS reactor.

Figure 4 shows the gravimetric CO-consumption rates over the prepared and the commercial LTS catalysts. The WGS reaction of a feed containing 62.5% H_2, 31.8% deionized H_2O and 5.7% CO was carried out at reaction temperature of 200–300 °C and space velocity of $10\,000\,h^{-1}$. The Cu-Zn/Al_2O_3 catalyst was reduced at 200 °C in a mixture of 2% H_2 in N_2 balance for 4.5 h and the Mo_2C catalyst was reduced at 400 °C under the flow of H_2 for 4.5 h. It was found that Mo_2C catalysts showed higher activity than the Cu-Zn/Al_2O_3 catalyst at temperatures above 260 °C. The catalytic activity of Mo_2C (catalyst D) increased progressively with increasing reaction temperature, and maximum activity was observed at 280–300 °C with a CO-consumption rate of more than 5.1 μmol/g/s. However, the Cu-Zn/Al_2O_3 catalyst displayed the

Table 1
Characteristics of commercial and prepared catalysts

Code	Catalyst formulation	Carburization temperature (°C)	BET surface area (m^2/g)	Total pore volume (cc/g)	Active metal surface area (m^2/g)
A	Cu-Zn/Al_2O_3	–	60	0.079	0.104
B	Mo_2C	615	48	0.028	–
C	Mo_2C	630	52	0.034	–
D	Mo_2C	640	61	0.036	0.129
E	Mo_2C	650	64	0.042	0.138
F	Mo_2C	660	44	0.024	–
G	Mo_2C	670	32	0.021	–

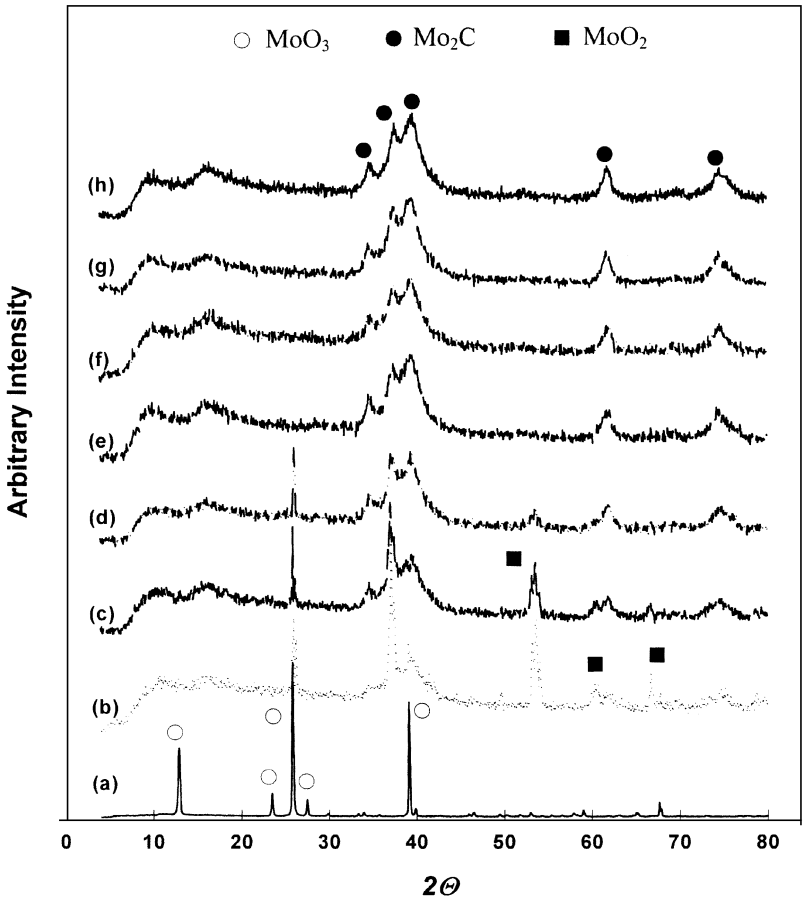

Figure 3. XRD patterns for molybdenum carbide catalysts with different carburization temperatures. (a) MoO_3 (b) Mo_2C −615 (c) Mo_2C −620 (d) Mo_2C −630 (e) Mo_2C −640 (f) Mo_2C −650 (g) Mo_2C −660 (h) Mo_2C −670.

highest activity at 260 °C with CO-consumption rate of 4.5 μmol/g/s.

Figure 5 represents the correlation of the CO-consumption rate with the carburization temperature of molybdenum oxides. The WGS reaction was carried out under the same reaction conditions as figure 4. The catalytic activities of molybdenum carbides were dependent on the carburization temperature. The activities

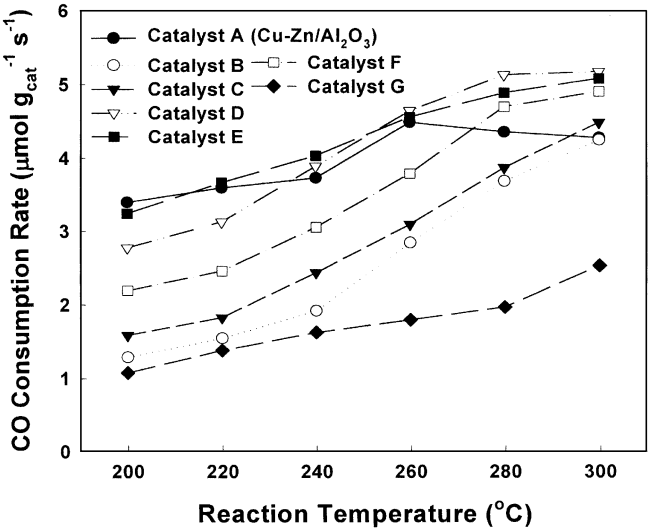

Figure 4. The gravimetric CO-consumption rates over the prepared (Mo_2C) and the commercial LTS ($Cu\text{-}Zn/Al_2O_3$) catalysts. Carburization temperature = 615–670 °C; space velocity = 10 000 h^{-1}; feed molar ratio = H_2 (62.5%), H_2O (31.8%), CO (5.7%).

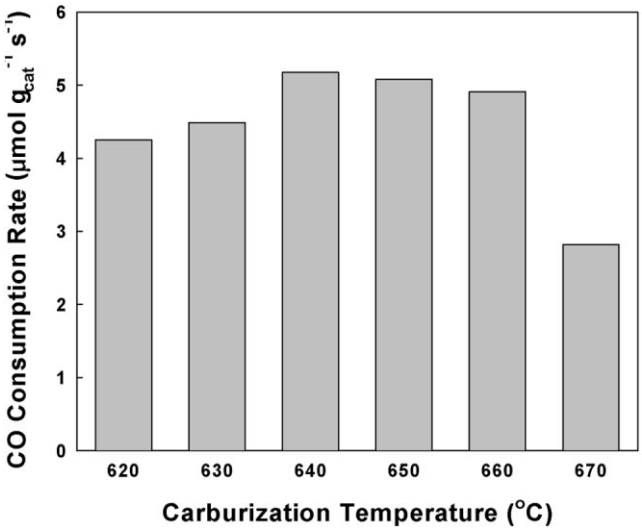

Figure 5. CO-consumption rates as a function of the carburization temperature of molybdenum oxide. Reaction temperature 300 °C; space velocity = 10 000 h^{-1}; feed molar ratio = H_2 (62.5%), H_2O (31.8%), CO (5.7%).

over molybdenum carbides catalysts follow the order

$$Mo_2C(640\,^{\circ}C) > Mo_2C(650\,^{\circ}C) > Mo_2C(660\,^{\circ}C) > Mo_2C(630\,^{\circ}C) > Mo_2C(615\,^{\circ}C) > Mo_2C(670\,^{\circ}C)$$

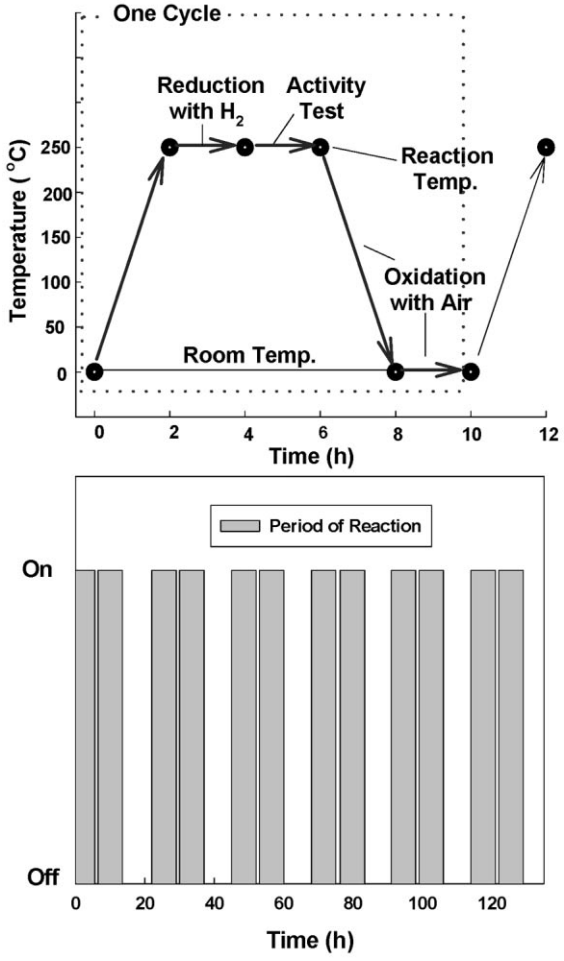

Figure 6. Thermal cycling runs with on/off repeated reactions during a time period of 130 h.

It was found that the optimum carburization temperature of molybdenum oxide for the WGS reaction was in the range of 640–650 °C. At carburization temperatures lower than 640 °C, carburization of molybdenum oxide will not be completed, whereas at higher temperatures, in excess of 650 °C, excess carbon deposits on the carbide systems, thereby resulting in low activity.

The thermal cycling runs were performed at the reaction temperature of 250 °C over a time period of 130 h. The procedures for thermal cycling run are summarized in figure 6. To change the reduction and oxidation conditions of catalysts, the switch of the electric furnace for heating the WGS reactor was repeatedly operated on/off with some intervals. Figure 7 shows the results of thermal cycling runs for WGS reaction over Cu-Zn/Al_2O_3 and Mo_2C (catalyst D)

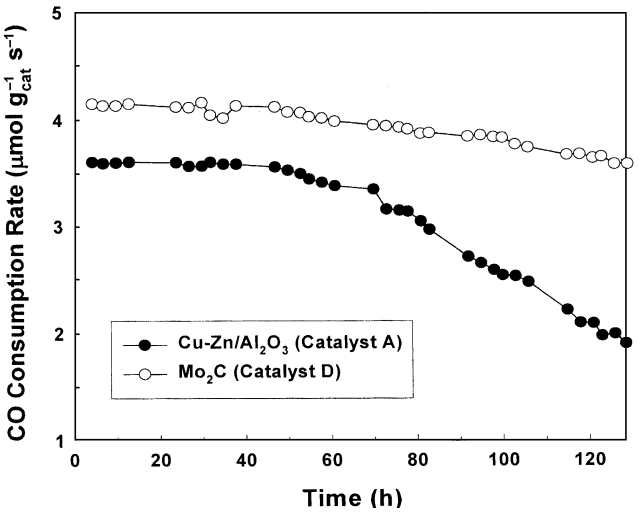

Figure 7. The results of thermal cycling runs for the WGS reaction over commercial LTS and Mo_2C catalysts. The runs were performed at the reaction temperature of 250 °C over a time period of 130 h.

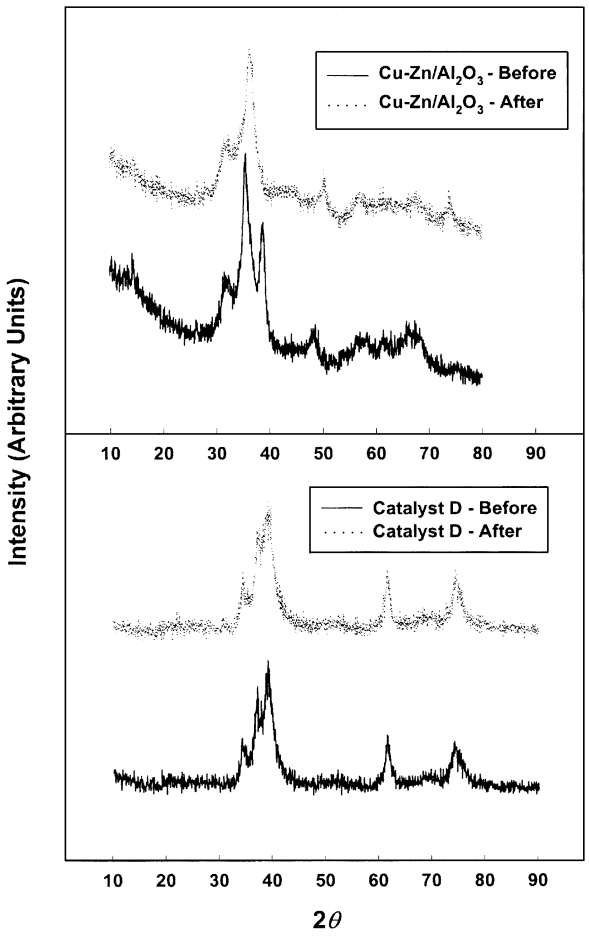

Figure 8. The XRD patterns of catalysts before and after the thermal cycling reaction. The runs were performed at the reaction temperature of 250 °C over a time interval of 130 h.

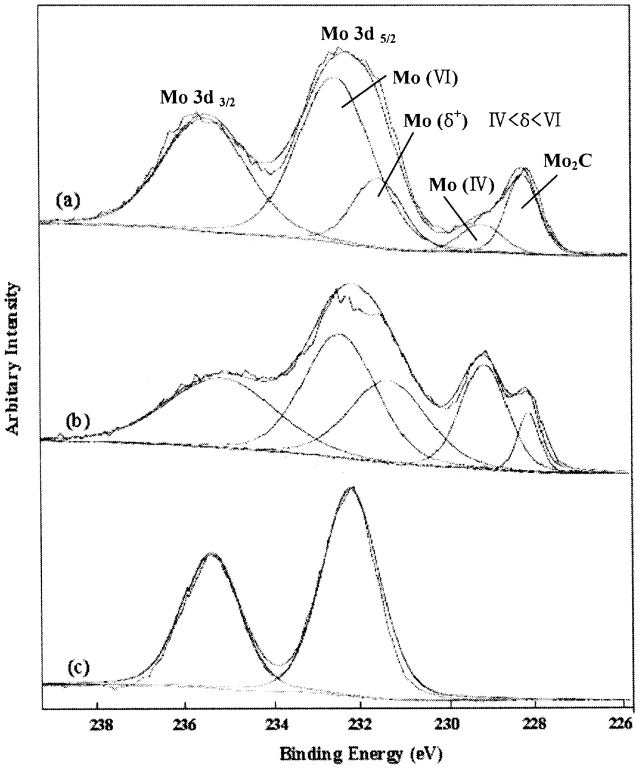

Figure 9. The XPS spectra of Mo_2C catalysts before and after the thermal cycling reaction. (a) Mo_2C after synthesis and air exposure at room temperature. (b) Mo_2C after H_2 treatment at 400 °C for 4.5 h and air exposure at room temperature. (c) Mo_2C after H_2 treatment at 400 °C for 4.5 h and then thermal cycling reaction at 250 °C for 130 h.

catalysts. It was found that the CO-consumption rate over Cu-Zn/Al_2O_3 and Mo_2C catalysts decreased progressively with time onstream. The CO-consumption rate of Mo_2C and Cu-Zn/Al_2O_3 catalysts after the thermal cycling reaction for 130 h decreased by 8 and 17% respectively. It was found that the Mo_2C catalyst showed higher stability than the commercial LTS catalyst during thermal cycling test.

X-ray diffraction patterns of the commercial LTS and Mo_2C (catalyst D) catalysts before and after the reactions are presented in figure 8. The used catalysts were recovered after the thermal cycling reaction at 250 °C for 130 h. There was no major change in the XRD patterns of the Mo_2C catalyst before and after the reaction. Only Mo_2C was present in the XRD patterns. Ledoux *et al.* [11–13] reported studies on the phase transition of the Mo_2C catalyst after air treatment and after catalytic use. They found from the XRD patterns that there was no change in the phase of Mo_2C after air treatment at room temperature, but the presence of Mo_2C and a small amount of MoO_3 were detected over the Mo_2C catalyst after air treatment at 350 °C for 14 h. They also reported that the oxide phase has disappeared and only Mo_2C was presented in XRD patterns of Mo_2C after air treatment at 350 °C for 14 h and *n*-hexane reaction by hydrogen at 350 °C for 72 h. It was impossible to distinguish between molybdenum carbide and molybdenum oxy-carbide (MoO_xC_y) using XRD analysis alone, due to the similarity of their XRD patterns. In this work, because the Mo_2C catalyst under thermal cycling run was alternately exposed at the states of oxidation and reduction, it was considered that the surface of the Mo_2C catalyst during thermal cycling run may be oxidized to molybdenum oxide. To elute the characteristics of Mo atoms on the surface of the Mo_2C catalyst, studies on XPS were investigated.

Figure 9 shows the XPS spectra of catalysts after synthesis and air exposure at room temperature, after H_2 treatment at 400 °C for 4.5 h and then after thermal cycling reaction at 250 °C for 130 h. Binding energy and relative percent of XPS peak for Mo_2C catalysts are summarized in table 2. The obtained XPS spectra were fitted using a nonlinear least square method with the convolution of Gaussian–Lorentzian functions [12,17]. It was identified that binding energies of Mo $3d_{5/2}$ for $Mo^{VI}(MoO_3)$, $Mo^{\delta+}(MoO_xC_y)$, $Mo^{IV}(MoO_2)$ and Mo_2C are 232.4, 231.4, 229.2 and 228.4 eV respectively, where δ is an intermediate oxidation states between IV and VI (IV $< \delta <$ VI) [11–13,19–21]. It was found that the XPS peak fitting gives 13.1 and 18.3% of surface Mo

Table 2
Characteristics of catalysts before and after the thermal cycling reaction

Catalyst	Condition	BET surface area (m^2/g)	Total pore volume (cc/g)	Active metal surface area (m^2/g)
A	Fresh	60	0.079	0.104
	Used	42	0.068	0.084
D	Fresh	61	0.036	0.129
	Used	53	0.031	0.104

Table 3
Binding energy and relative percent by XPS for the molybdenum carbide catalysts tested

Catalyst	Mo $3d_{3/2}$	Mo $3d_{5/2}$			
		Mo^{VI} (MoO_3)	$Mo^{\delta+}$ (MoO_xC_y)	Mo^{IV} (MoO_2)	Mo_2C
Binding energy (eV)	235.3	232.4	231.4	229.2	228.4
Mo_2C[a]	–	62.5%	18.3%	6.1%	13.1%
Mo_2C[b]	–	41.8%	29.9%	22.2%	6.1%
Mo_2C[c]	–	100%	–	–	–

[a]Mo_2C after the synthesis and air exposure at room temperature.
[b]Mo_2C after the H_2 treatment at 400 °C for 4.5 h and air exposure at room temperature.
[c]Mo_2C after the H_2 treatment at 400 °C for 4.5 h and then thermal cycling reaction at 250 °C for 130 h.

atoms engaged in Mo_2C and $Mo^{\delta+}$ respectively, 6.1% of surface Mo atoms corresponding to $Mo^{IV}(MoO_2)$ and 62.5% of surface Mo corresponding to $Mo^{VI}(MoO_3)$ in the Mo_2C catalyst after the synthesis and air exposure at room temperature. It was found that $Mo^{VI}(MoO_3)$ and Mo_2C phase on the surface of the catalyst after the H_2 treatment at 450 °C for 4 h and air exposure at room temperature decreased from 65.5 to 41.8% and from 13.1 to 6.1% respectively. $Mo^{\delta+}$, Mo^{IV} and Mo_2C phase on the surface of the Mo_2C catalyst after the H_2 treatment at 450 °C for 4 h and thermal cycling reaction at 250 °C for 130 h was not observed. $Mo^{VI}(MoO_3)$ phase on the surface of the Mo_2C catalyst after the reaction increased from 62.5 to 100%. It was found from XPS peak fitting that most of the Mo atoms present on the surface of the Mo_2C catalyst after the thermal cycling reaction were $Mo^{VI}(MoO_3)$.

The characteristics of the catalysts before and after the thermal cycling reaction for 130 h are summarized in table 2. BET surface area of Mo_2C (catalyst D) and Cu-Zn/Al_2O_3 catalysts after the thermal cycling reaction decreased by 13 and 29% respectively. Active metal surface of Mo_2C and Cu-Zn/Al_2O_3 catalysts after the reaction decreased by 19 and 21% respectively. In our previous work [6–9], we reported that Cu-Zn/Al_2O_3 catalyst was deactivated by sintering of active metal during the thermal cycling test. It was interpreted that the BET surface area of the Mo_2C catalyst after the thermal cycling reaction decreased by changing $Mo^{\delta+}(MoO_xC_y)$, $Mo^{IV}(MoO_2)$ and Mo_2C on the surface of the Mo_2C catalyst to MoO_3, thereby giving low activity for the WGS reaction, and causing the deactivation of the Mo_2C catalyst. It was concluded that the deactivation of the Mo_2C catalyst during the thermal cycling run for WGS reaction was caused by the transition of $Mo^{\delta+}$, Mo^{IV} and Mo_2C on the surface of the Mo_2C catalyst to $Mo^{VI}(MoO_3)$ with the reaction of H_2O in reactants.

4. Conclusions

To develop a high-performance LTS catalyst for fuel cell–powered vehicle applications, the WGS reaction over molybdenum carbide prepared by temperature-programmed carburization of molybdenum oxide was investigated. It was observed that the activity of the molybdenum carbides was greatly dependent on the carburization temperature. The catalytic activities of molybdenum carbides catalysts follow the order

$$Mo_2C(640\,^\circ C) > Mo_2C(650\,^\circ C) > Mo_2C(660\,^\circ C) > Mo_2C(630\,^\circ C) > Mo_2C(615\,^\circ C) > Mo_2C(670\,^\circ C)$$

Optimum carburization temperature for preparing the Mo_2C catalyst for the WGS reaction was in the range of 640–650 °C.

It was found that Mo_2C catalysts displayed reasonably good activity than commercial Cu-Zn/Al_2O_3 catalyst. It was also found that the Mo_2C catalyst showed higher stability than the commercial LTS

catalyst during the thermal cycling test. It was concluded from XPS spectra and the thermal cycling reaction that the deactivation of the Mo_2C catalyst may be caused by the transition of $Mo^{\delta+}(MoO_xC_y)$, $Mo^{IV}(MoO_2)$ and Mo_2C on the surface of the Mo_2C catalyst to $Mo^{VI}(MoO_3)$ with the reaction of H_2O in reactant.

The results suggest that the Mo_2C catalyst is an attractive candidate for the alternate $Cu\text{-}Zn/Al_2O_3$ catalyst for automotive applications, even though this catalyst was slowly deactivated during the thermal cycling run.

Acknowledgment

Funding for this work from KIST is greatly appreciated. We thank the research group on gasoline reformer in KIST for helpful discussions.

References

[1] Arthur D. Little Inc., Multi-Fuel Reformers for Fuel Cells Used in Transportation, Multi-fuel Reformers Phase I, Final Report, DOE/CE/50343-2 (1994).
[2] D.J. Moon and J.W. Ryu, Catal. Lett. 89(3–4) (2003) 207.
[3] D.J. Moon, Jong Woo Ryu, Sang Deuk Lee and Byoung Sung Ahn, Korean J. Chem. Eng. 19(6) (2002) 921.
[4] W. Ructtinger, O. Ilinich, R.J. Farrauto, J. Power Sources 52 (2003) 1.
[5] L. Lloyd, D.E. Ridler and M.V. Twigg, *Catalyst Handbook*, 2nd edn (Wolfe Publ. Ltd., UK, 1989), p. 308.
[6] D.J. Moon, J.W. Ryu, S.D. Lee and B.S. Ahn, *2002 Fuel Cell Seminar*, Palm Springs, USA, 2002, p. 348.
[7] D.J. Moon, K. Screekumar, S.D. Lee, B.G. Lee and H.S. Kim, Appl. Catal. A Gen. 215 (2001) 1.
[8] L. Thompson, J. Patt, D.J. Moon and C. Phillips, Transition metal carbides and nitrides and borides useful as water gas shift catalysts, U.S. Patent 0013221 A_1 (2002).
[9] J. Patt, D.J. Moon, C. Phillips and L. Thomson, Catal. Lett. 65 (2000) 193.
[10] J.S. Lee, S.T. Oyama and M. Boudart, J. Catal. 106 (1987) 125.
[11] M.J. Ledoux, C. Pham-Huu, A.P.E. York, E.A. Blekkan, P. Delporte and P. Del Gallo, *The Chemistry of Transition Metal Carbides and Nitrides* (New York, USA, 1993), p. 373.
[12] M.J. Ledoux, C. Pham-Huu, H. Dunlop and J. Guille, *Proc. 10th Int. Congr. on Catalysis* Budapest, Hungary, 1992, p. 965.
[13] M.J. Ledoux, C. Pham-Huu, J. Guille and H. Dunlop, J. Catal. 134 (1992) 380.
[14] J.M. Muller and F.G. Gault, Bull. Soc. Chim. Fr. 2 (1970) 416.
[15] R.B. Levy and M. Boudart, Science 181 (1973) 547.
[16] A. Holmgren, F. Azarnoush and E. Fridell, Appl. Catal. B: Environ. 22 (1999) 49.
[17] C. Song, Catal. Today 77 (2002) 17.
[18] SSI Science Inc., Hand Book of X-Ray Photoelectron Spectroscopy, SSI scientific 2803-S spectrometer (2000) 226.
[19] L. Bugyi, A. Oszko and F. Solymosi, Surf. Sci. 461 (2000) 177.
[20] C. Gaillard, N. Chevarier and C.D. Auwer, J. Nucl. Mater. 299 (2001) 43–52.
[21] J.G. Choi and L.T. Thompson, Appl. Surf. Sci. 93 (1996) 143–149.